ZIBELINE INTERNATIONAL™ PUBLISHING

Water Conservation and Management (WCM)

DOI: http://doi.org/10.26480/wcm.01.2026.127.138

ISSN: 2523-5664 (Print)
ISSN: 2523-5672 (Online)
CODEN: WCMABD

RESEARCH ARTICLE

MATHEMATICAL MODELING FOR SUSTAINABLE WATER MANAGEMENT OF KARAKATA GROUNDWATER DEPOSITS

Saydulla Khushvaktov[a], Botirjon Abdullaev[b*], Erkin Anorboev[a], Alisher Mirsaatov[a], Bakhrom Abdullaev[a,b], Utkir Mardiev[a], Dilnavoz Kholjigitova[a], Munavvar-Bonu Turaeva[a], Marjona Gofurjonova[a]

[a]State Establishment "Institute of Hydrogeology and Engineering Geology", Tashkent, Uzbekistan
[b]Tashkent Institute of Irrigation and Agricultural Mechanization Engineers, National Research University, Tashkent, Uzbekistan
****Corresponding Author Email: botirjon.dadajonovich@tiiame.uz***

Article History:

Received 23 February 2026
Revised 2 March 2026
Accepted 16 March 2026
Available online 30 March 2026

ABSTRACT

This study presents a numerical assessment of groundwater flow and filtration properties of the Senonian–Lower Eocene aquifer complex within the Karakata artesian basin (Uzbekistan). The research is based on the interpretation of long-term operational data, well test results, and regime observations obtained under conditions of incomplete and heterogeneous hydrogeological information. Key filtration, water conductivity, elasticity, and piezo conductivity parameters were estimated using analytical approaches and refined through inverse problem solutions.A single-layer groundwater flow model with spatially heterogeneous hydraulic properties was developed using the MODFLOW code. The model incorporates major structural features of the basin, including tectonic fault zones acting as pathways for additional groundwater recharge and discharge. Model calibration was performed through stationary and transient inverse simulations, achieving good agreement between observed and simulated piezometric heads, with deviations generally within ±5 m.The results indicate that the aquifer complex is predominantly confined and exhibits pronounced lateral heterogeneity in hydraulic conductivity. Long-term exploitation has been sustained mainly by dynamic flow reserves and elastic storage, with a significant contribution from fault-controlled inflow from the Paleozoic basement. The estimated dynamic groundwater reserves are lower than previously reported values.The developed model provides a reliable framework for groundwater balance assessment, forecasting of aquifer response to pumping, and sustainable groundwater resource management in arid regions.

KEYWORDS

Hydraulic conductivity, Filtration heterogeneity, MODFLOW, Inverse modeling, Groundwater balance, Tectonic faults, Artesian basin, piezometric head, Aquifer parameters, Numerical simulation, Groundwater resources.

1. INTRODUCTION

The current state development of modeling hydrogeological processes has been achieved thanks to fundamental research results on numerical modeling of geofiltration and geomigration processes in complex hydrogeological conditions, the creation of automated modeling systems, and information support for hydrogeological research (Henshaw et al., 2000; Polshkova, 2023; Zaborova et al., 2020, Hushvaktov et al., 2021).In this regard, it is worth noting the research related to modeling the dynamics of water and mass transfer in the underground hydrosphere the creation of automated technologies for modeling hydrogeological systems - Choi and Mantilla (Choi and Mantilla, 2015; Harne et al., 2006; Shestakov and Nevecherya, 2009; Akhtar et al., 2020; Funikova et al., 2022; Abdullaev et al., 2023).The research and others, the information support of large hydrogeological projects and the creation of constantly operating models of large hydraulics (Chesnaux et al., 2011; Hushvaktov et al., 2021; Chen et al., 2022; Zakir-Hasan et al., 2025;Jamali et al., 2025). One of the modern methods of mathematical modeling is the use of artificial intelligence elements for managing complex dynamic objects, which can include hydrogeological objects (HGO) capable of functioning under conditions of uncertainty in the mathematical description of the management object. The significant instability of processes in hydrogeological objects, consisting in the change in the characteristics of the process over time, as well as their weak reproducibility, require the application of new modern management principles - intelligent management algorithms, especially if management is carried out on a real time scale. In some countries, modeling results are needed on issues such as groundwater depletion and restoration, water diversion, and the impact of agriculture, and these areas are currently being addressed (Kashavarov, 1998; Long et al., 2020).Mapping and modeling are now widely used to study groundwater and surface water resources and their relationships (Carrera et al., 2005; Brodie et al., 2007).In many regions of Uzbekistan, groundwater or the impact of economic sectors on groundwater has been studied using numerous models (Rasouli et al., 2025; Hafezifar and Shourian, 2025). However, there is still insufficient information on groundwater movement, deposits, and the application of modern modeling methods.

1.1. Purpose

The hydrogeological conditions of the Republic of Uzbekistan are

Quick Response Code	Access this article online	
	Website: www.watconman.org	**DOI:** 10.26480/wcm.01.2026.127.138

Cite The Article: Saydulla Khushvaktov, Botirjon Abdullaev, Erkin Anorboev, Alisher Mirsaatov, Bakhrom Abdullaev, Utkir Mardiev (2026). Mathematical Modeling for Sustainable Water Management of Karakata Groundwater Deposits. Water Conservation and Management, 10(1): 127-138.

distinguished by their complexity and diversity, which are due to the physical-geographical structure and structural plan of its western and eastern parts.In mining structures, cracked and porous groundwater, predominantly of shallow circulation, is developed. In the depressions of the mountainous folded region, pressure-bearing water complexes lie, forming foothill intermountain artesian basins. In the mountainous folded region, a thick zone of active water exchange is observed in the intersection of the deposits of artesian basins and groundwater basins, and as a result, fresh and slightly saline waters are formed here.

A characteristic feature of the plain-platform hydrogeological region is the development of large artesian basins composed of aquifers and water-resistant layers of the Paleogene, Cretaceous, and Jurassic. Saline, salty, and brackish groundwater is formed in their cross-sections. Fresh groundwater is extremely scarce here.Groundwater is confined to collectors of various origins in all stratigraphic subdivisions participating in the geological structure of the republic's territory, forming aquifers and complexes, local aquifers, and cracking zones. The thick, visible at considerable distances, clay, marl, and halogen layers are water-resistant, determining the hydrodynamic characteristics of various parts of the hydrogeological section (Abdullaev et al., 2023).

In the territory of the Republic of Uzbekistan, drinking and technical water deposits are associated with aquifers and complexes, distributed within the limits of:

- modern and buried river valleys.
- in large and small alluvial fans and terrestrial deltas of foothills.
- in intra-mountain, foothill, inter-aerial, and inter-aerial depressions.
- in artesian basins.
- in sandy massifs of deserts and semi-deserts.
- in river and canal lenses.
- in limited structures or masses of fractured-karst rocks and tectonic disruption zones.

Such a classification of deposits reflects the main hydrogeological features of the formation and distribution of groundwater in the territory of the Republic.

The modern synclinal structure of the Karagatin Basin was carried out against the backdrop of the active manifestation of alpine tectogenesis, productive aquifers complex conditionally associated with the age-related undifferentiated deposits of the Lower Eocene and Upper Cretaceous (Funikova et al., 2022).

It reflects the different intensity of submergence of Paleozoic foundation blocks formed by an uneven network of tectonic faults (faults), which have predominantly sub meridional and sub latitudinal directions. The greatest descent velocity of these blocks led to the maximum complex capacity of 150 meters or more in the central part of the depression, where the complex is submerged to a depth of 300-400 meters from the earth's surface. The depth of its occurrence and, accordingly, the thickness decrease from the center to all directions towards the sites where the complex emerges to the surface or to the boundaries of its junction with the Paleozoic uplifts (Figure 1) - the formation of the aquifer complex occurred together with the formation of Senonian and Lower Eocene deposits.

The material of these deposits was water-resistant clays of the Turonian stage, on which sands with varying amounts of clay material were deposited by paleo flows from the mountain rim.

During this entire geological period, groundwater movement occurred from mountain ranges to the lowest northern and central parts of the depression, where it intensively evaporated. In subsequent geological epochs, subsidence of the horizon occurred, which was covered by water-resistant sediments of mergels and clays. However, the process of groundwater supply, transit, and discharge has been preserved with the difference that discharge by wedging groundwater to the surface and subsequent evaporation has been replaced by discharge by flowing into the above-lying sediments through the weakened zone of the roof, adjacent to the fault zones.

In turn, the ascending flows of groundwater, through the thickness of overlying precipitation, reach the current position of the earth's surface, forming significant areas of saline spaces as a result of the evaporation of decreasing groundwater. This process is convincingly confirmed by the depth of the established groundwater level of the complex when opened by wells, when it is recorded at depths several tens of meters below the ground level in areas close to the outcrops of the complex deposits to the surface and exceeds the ground level by 30-50 meters in the central and northern parts of the basin. The pressure height above the layer roof increases in the same direction from tens to hundreds of meters (around 300m in the center of the depression).

This nature of the groundwater formation process is confirmed by piezoisohypsic maps compiled during exploration and exploitation. From these maps, it follows that the main part of the underground flow is formed not from the local mountain outcrop of the Karakata depression itself, but beyond its eastern boundaries due to part of the underground flow formed within the southern and northern slopes of the Northern and Southern Nuratau, Aktau ranges, the northern slope of the Karatau range, i. e., the eastern and southeastern inflow of underground waters from the Nurota and Arnasai depressions is predominant.

The map of water mineralization of the complex (Telyma et al., 2023), which clearly shows an increase in mineralization from the east and southeast in the northwest directions, testifies to the manifestation of precisely this process. In the northern and central parts of the Karakata Depression, the Senonian-Lower Eocene sedimentary aquifer complex is undoubtedly fed by numerous fault zones by underground waters from the fractured zones of the Paleozoic foundation.

- a productive water-bearing complex that has been intensively exploited for more than 50 years, characterized by sharp heterogeneity in plan and section in terms of filtration. It represents the interlayering of layers and layers of sandstones with sandy-stone alaurolites. Due to their varying permeability when opening with wells, the latter are characterized by flow rates from units to 30-40 l/s during testing, primarily at depths from 3-10 m to 30-40 m.

The specific flow rates of wells are 0.3-1.5 l/s per meter of depression. In addition to the permeability of the tested sediments, well productivity depends on their position relative to the water-conducting faults and the degree of imperfection of its filter equipment relative to the full capacity of the water-bearing complex. Analysis of information on wells drilled and tested at different times within the Karakata Basin.

They indicate that the tested well interval (filter length) across all wells is no more than 20-30 meters, with the total complex capacity reaching 100-150 meters.

The above-mentioned features of the formation of groundwater of the considered complex, its distribution, and indirect indicators of water permeability (specific well rates) allow us to draw the following conclusions:

- the well-tested part of the water-bearing complex (layer) in the section can be considered in most of the basin territory as a pressure layer, the thickness of which is limited by the length of the filter. The weak interaction of wells equipped with filters for adjacent intervals with the tested material during short-term testing demonstrates this approach.

- for wells located near the development of fault strips of the Paleozoic foundation, through which the upward filtration of groundwater (unloading) of all complexes (from the Paleozoic to the Quaternary) is carried out, the tested aquifer of the Senonian-Lower Eocene aquifer complex can be considered as quasi-pressurized (pressurized with flow through the separating layers);

- since in the conditions of operation of various intervals of the water-bearing complex, the full capacity of the complex is involved in the zone of influence and feeding of water intakes, in addition to the geofiltration indicators of the tested layers, the water permeability of the complex to its full capacity must also be characterized.

Therefore, the interpretation of the available information on testing the water-bearing complex of calculated parameters is aimed at the following:

- preliminary assessment of the water conductivity parameters of the complex; in general, for the basin (deposit);
- assessment of the water conductivity and filtration parameters of the tested intervals.
- assessment of the complex's water conductivity and elasticity.

From the above, it is evident that the application of modeling methods, which is one of the types of classical synthesis, involves representing complex systems as an interconnected set of simple objects, the models of which are known and well-studied and are oriented towards solving one-

sided problems for certain typical hydrogeological conditions. In this case, the main attention was paid to the models of hydrogeological processes, and representations of natural factors played a supporting role.

The contradictions between the complexity of real objects and the possibilities of modeling were eliminated, on the one hand, by schematizing hydrogeological conditions (companied processes were ignored, interaction with the environment was simplified, the heterogeneity of natural factors was smoothed out, etc.), and on the other hand, by reducing the requirements for the adequacy of models, the accuracy and completeness of initial data, etc. This naturally reflected on the quality of the results obtained. These assumptions often lead to the fact that classical methods in practice do not provide the specified management quality indicators.

All this necessitates the modification and development of new methods and algorithms for solving problems of managing complex objects, to which the natural object of hydrogeological objects - groundwater deposit (GWD) - belongs.

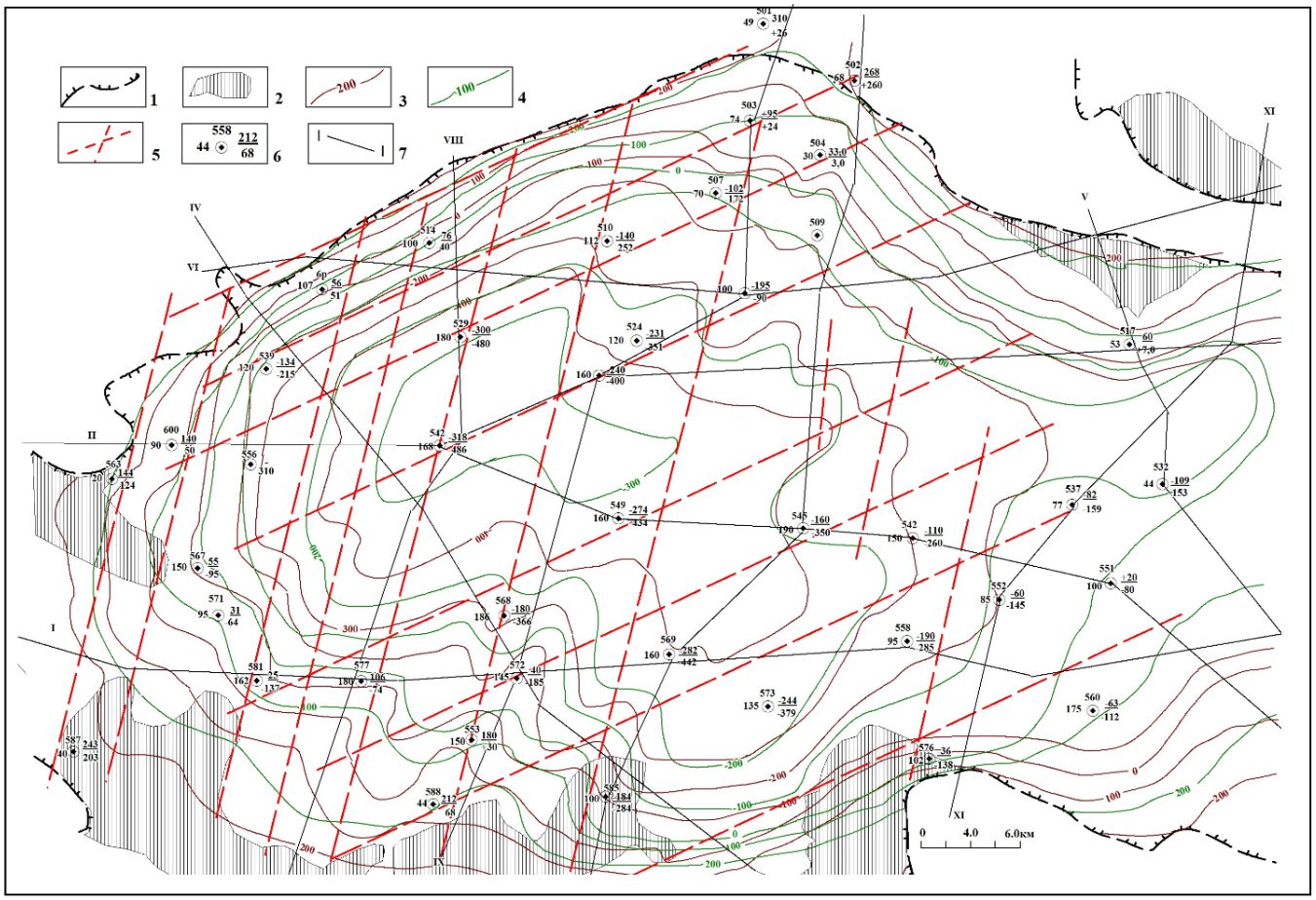

Figure 1: Structural map of the Karakata GWD. 1 - distribution boundary of the Senonian-Lower Eocene aquifer complex; 2 - outcrops of the Senonian-Lower Eocene aquifer complex; 3 - water-bearing complex sole isolines; 4 - water-bearing complex roof isolines; 5 - Predicted position of fault disruptions that controlled the formation conditions of Senonian-Lower Eocene deposits and associated groundwater; 6 - well above - number; on the left - water-bearing complex capacity; on the right - absolute marks: - in the numerator - roofs; - in the denominator - bottoms; 7 - lines of hydrogeological sections of the Aksai HGP (1969).

2. Methodology

The results of testing imperfect wells in terms of their degree of opening served as a basis for preliminary assessment of the water permeability coefficient characterizing the well's prefiltration zone ( ). This value, attributed to the unit length of the filter ( ), allows us to estimate the approximate filtration coefficient of the complex deposits and, with its known power ( ), to arrive at the total value of the water permeability coefficient ( ). This approach to preliminary assessment of water conductivity parameters has been tested in numerous facilities over the past 10 years and has shown a sufficiently high approximation to real parameters. The results of calculating water permeability according to the methodology are presented in Table 1. They are close to the values of individual interval parameters obtained during testing at different sites using other calculation methods (≈300 m2/day). The coefficients of the established elastic water yield, calculated according to the approximate dependence, taking into account the depth of submersion of the reservoir, the pressure above its roof, and the initial water yield of the reservoir in a pressure-free state, should be approximately at depths of: 100 m - ≈0,01; 200 m - ≈0,005; 300 m - ≈0,003. The piezo conductivity coefficients are estimated at ≈1-5×105 m2/day.

Table 1: Preliminary calculation of water permeability based on well sampling data Karakata Basin

№ well	q, l/s	kl=150* q	l	k=kl/l	M	km=m*k
5(1)	1.48	222	17.25	12.87	28.03	361
7	0.29	43.5	14.5	3	106	318
8(1)	0.26	39	29	1.34	106	142.0
6(1)	0.4	60	22.7	2.64	106	280.00
9(1)	0.2	30	17.7	1.69	106	179.0
9(1)	0.25	37.5	17.7	2.12	106	224.00
10	0.65	97.5	39.6	2.46	160	394.0
12pr1	1.32	198	27.15	7.29	74	539.4
503	1.74	261	42.8	6.10	74	451.4
568	0.08	12	18	0.67	186	124.62
569	0.74	111	21	5.29	160	846.4
577	1.5	225	19	11.84	76	800

Table 1(Cont.): Preliminary calculation of water permeability based on well sampling data Karakata Basin						
585	0.33	49.5	6	8.25	100	825
514	1.49	223.5	21	10.64	(34) 100	361
516	0.64	96	22	4.36	60	261.6
517	0.87	130.5	31	4.21	53	223.13
518	1.18	177	79	2.24	110	246.4
524	1.5	225	30	7.5	(92) 120	690
542	1.3	195	20	9.75	(60) 168	585
545	0.99	148.5	22.6	6.57	(90) 190	591
558	1.55	232.5	25	9.3	(72) 95	669
559	0.3	45	16	2.8	80	224
567	1	150	25	6.0	100	600
573	0.47	70.5	17	4.15	135	560.25
583	0.2	30	10	3	150	450
590	0.87	130.5	21	6.2	80	496
6s-re	0.546	81.9	30	2.73	100	273
1re	2.44	366	29	12.62	40	504.8
2v	3.57	535.5	24.0	22.3	40	892.0
3v	2.58	387.0	17.0	22.76	40	910.0

Based on the results of experimental bush releases and their interpretation, it was established that:

- The aquifer is pressurized, heterogeneous in elasticity, which is reflected in the characteristic graphs of downward tracking over time. Analysis of tracking graphs ($S-lgt, lgS-lgt, S/Q-lgt, lgS/Q-lgt$) allows us to confidently identify the elastic regime stage, which reflects the ultimate elasticity of the reservoir, transitioning from a pseudo-stationary stage to a stage reflecting the actual elasticity of the reservoir. Within this stage, a certain decrease in the rate of pressure reduction compared to the reference pressure is planned due to possible additional reservoir power sources, which may be, under given conditions, the overflow from adjacent aquifers or the natural flow of groundwater within the reservoir itself.
- Unfortunately, the short duration of release (7 days) did not allow for sufficiently confident confirmation of these processes. The identified features of the manifestation of pressure decrease under the influence of discharge are reflected in the applied methods for calculating the parameters of the aquifer.

Interpretation was performed by:

- time tracking method (Jacob method), based on the analysis of graphs in $S-lgt, S/Q-lgt$ coordinates;
- by the method of Hanthus-Jacob reference curves, based on the analysis of tracking graphs in the coordinates $lgS-lgt, lgS/Q-lgt$.

The results of parameter calculations are presented in Table 2. In general, they characterize close values of reservoir parameters, which, however, can lead to significant differences in calculated depressions depending on the acceptance of the hypothesis about the homogeneity or heterogeneity of the reservoir by elasticity, as well as the hypothesis about the presence of additional reservoir supply (in addition to elastic reserves) due to overflow and natural flow or its absence. Based on the above parameters, the formation can be grouped as follows

Table 2: Values of calculated filtration parameters for various hydrodynamic diagrams

No	Hypothesis	***km*, m²/day**	***a*, m²/day**	***B*, m**
1	The layer is heterogeneous in elasticity, with additional feeding.	196.54-202.97	2.7-3.5·10⁵	2075
2	The layer is homogeneous in elasticity, with no additional power supply.	299.07-303.65	3.52·10⁶-3.6·10⁶	-

Due to the insufficient validity of hypothesis 1, which can only be proven by long-term releases, let's focus on hypothesis 2, considering these parameters not as real but as generalized parameters reflecting not only the filtration characteristics of the reservoir but also boundary conditions (particularly, the possible influence of developed fault disruptions here), as well as additional feeding.

Therefore, the basis is the reservoir parameters obtained from a sufficiently convincing time tracking graph, which also takes into account the change in flow rate during production (graph in $S/Q-lgt$ coordinates). The calculated parameters of the reservoir are km - 300 m²/day, and - 3.6·106 m²/day.

Thus, the water permeability coefficients in the tested horizon intervals are presented as sufficiently stable. They fully correspond to the values reflected in the Karakata Basin Water Conductivity Map (Figure 2), which is placed in the filtration basis of the mathematical model.

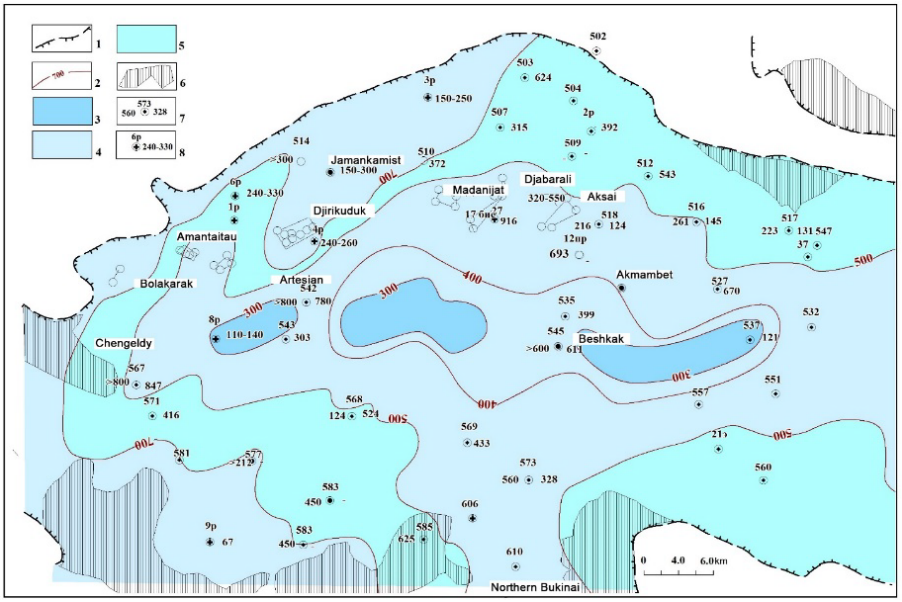

Figure 2: Map of water permeability of the Senonian-Lower Eocene aquifer. 1 - distribution boundary of the Senonian-Lower Eocene aquifer complex; 2 - isolines of the water conductivity coefficients of the Senonian-Lower Eocene aquifer complex, m2/day; 3 - water permeability less than 300 m2/day; 4 - also - 300-500 m2/day; 5 - also - 500-700 m2/day; 6 - outcrops of the Senonian-Lower Eocene aquifer complex; 7 - well: at the top, on the left - water permeability coefficient according to the approximate dependence, on the right - water permeability coefficient according to the Aksai Hydraulic Power Plant, m2/day; 8 - wells of the regime network of Navoi and Bukhara hydrogeological stations; at the top - well number; on the right - water permeability coefficient based on the results of operation of Bukhara hydrogeological stations.

The calculation of water conductivity parameters in the Karagatin groundwater field was carried out based on the lowering data in the wells of the regional observation network and the operational flow rate of group and single water intakes. It should be noted that there is no complete data The operation of the Karagatin underground water field began in 1955 with a total withdrawal of 140 l/s. The total flow rate of water intakes during the period from the start of operation to 1959 increased to 645 l/s. Before this period, the flow rates of individual water intakes were not measured. Nevertheless, there is data on the total intake for all water intakes for practically all years of operation, starting from 1955 (Table 3).

on the costs of operating wells: group water intakes and single wells for the entire period of operation of the Karagatin field; reports provide measurements of water intake rates for individual years.

For the period 1959-1968, flow measurements are available for individual water intakes: Balakarak, Artesian, 17-bis, Aksai. From 1969 to 1990, there is fragmented information on the flow rates of individual water intakes. Starting from 1990, there are actual costs for all water intakes for the period 1990-1993, 1996, 2003-2006. From 2007 to 2018, there is only information on the total water intake for the Karakata GWD.

Table 3: Total water intake from operating water intakes Senon-Lower Cennic aquifer complex of Karagatin artesian basin

Years	Total productivity of water intakes		Years	Total productivity of water intakes	
	thousand m^3/day	l/s		thousand m^3/day	l/s
1955	12.096	140	1996	65.7	760.4
1959	55.728	645	1999	59.46	688.2
1960	63.504	735	2000	52.66	609
1964	70.848	820	2002	44.55	515
1970	53.75	680	2004	47.0	544
1975	63.07	730	2006	38.15	442
1980	76.03	880	2007	37.8	437.5
1984	98.5	1140	2009	37.8	437.5
1985	105.41	1220	2010	38.66	447.45
1986	100.22	1160	2011	44.31	435.5
1987	107.31	1242	2012	37.67	436
1988	107.31	1242	2013	44.92	519.9
1989	117.91	1365	2014	40.09	464
1990	118.9 (approved)	1376	2015	37.75	437
1991	118.93	1376	2016	37.75	437
1992	92.84	1074	2017	38	439
1993	76.52	886			

Since the assessment of parameters was carried out based on operational data, starting from 1960, it was necessary to determine the flow rate of each water intake for a given period of time. Taking into account that such data are absent, and only a total sample is available for the entire field, an approximate recalculation of the flow rate of each water intake was carried out. For those group water intakes for which actual data were not available, the total flow rate of the Karakata field water intakes for each year of operation was distributed in percentage terms, similar to 1990-1993.

Since the influence of all operating wells must be taken into account when calculating the parameters, it is necessary to specify the costs of all single water intake wells at each calculation step. The costs of single water intakes were recalculated for all years of operation in percentage terms, similar to 2003.

The performed calculations of the hydrogeological parameters of the tested layers and the complex as a whole, despite a number of accepted conventions related to the lack of reliable data on water intake discharges, pressure values, and the operating time of each intake, generally showed sufficiently real figures for filtration and water permeability coefficients. However, the reliability of such figures cannot be confirmed due to the lack of reliable information on pilot tests and operational results (Figure 3)

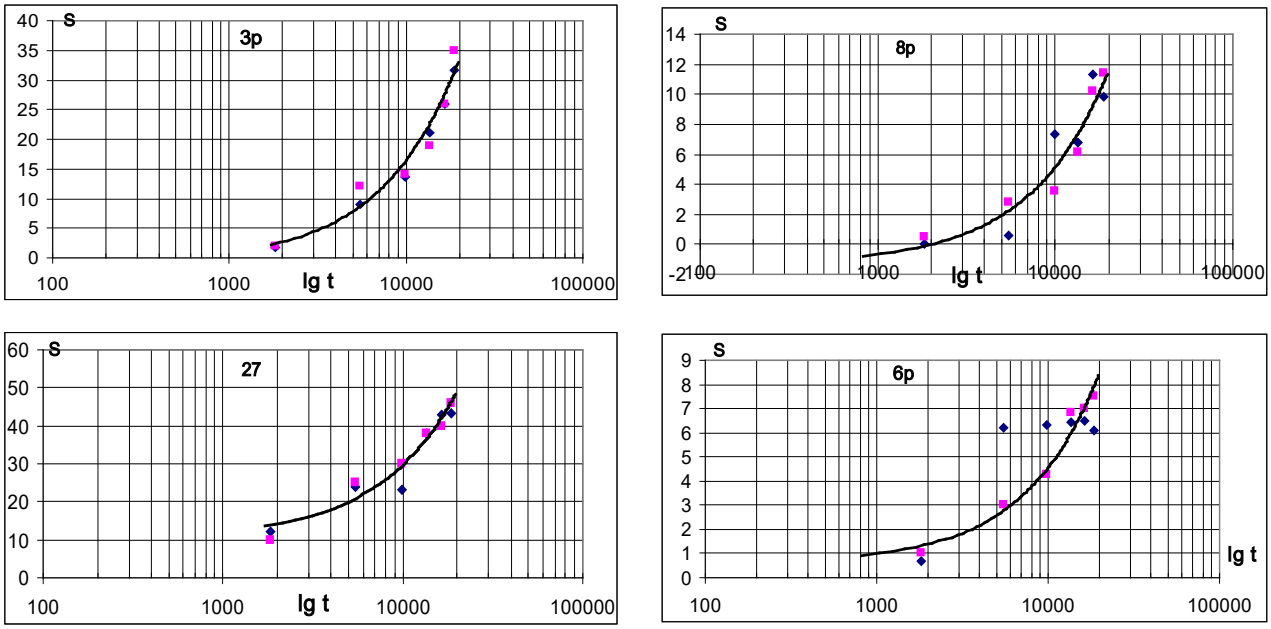

Figure 3: Graphs of temporary tracking of actual and calculated drawbacks based on regime well data

The geofiltration structure of the aquifer complex in plan is reflected in the water conductivity map (Figure 2). On the map, with some assumptions, zones with water conductivity coefficients are distinguished:

- less than 300 m2/day adjacent to the outcrops of the complex deposits to the surface;
- 300-500 m2/day, bounding the boundaries of the filtration flows from the Nuratov and Karatau sides;
- more than 500 m2/day, allocated in the central and northern parts of the deposit, within which the deposits of the complex have existed throughout the entire post-sedimentation period of its geological development history under conditions of upward discharge of groundwater along weakened zones of tectonic disturbances. Overall, the planned filtration heterogeneity of the complex deposits obeys and reflects the influence of tectonics in the form of a block structure. Deposits within each block, depending on their location, are characterized by varying permeability.

The geofiltration structure of the aquifer complex in the section has not been identified. As a rule, tested wells characterize the upper exposed part of the water-bearing complex within the filter length intervals. Usually, it does not exceed 25-30 m, i.e., it constitutes 20-25% of the total complex capacity. It can be conditionally assumed that the aquifer complex consists of 4-5 layers similar to those unearthed in the upper part of the complex. The participation of the entire capacity of the complex in the natural, and then also in the artificial, forced operation, discharge of groundwater, is undeniable.

Therefore, the water-bearing complex can be conditionally divided into 4-5 layers characterized by water permeability similar to the upper, tested layer.

The modeling of filtration utilized the ModFlow software package of the American Geological Society. The use of this software for modeling the Karagatinskoye field made it possible to schematize the aquifer as single-layer due to the flow between layers, with planned filtration heterogeneity.At the first stage of modeling, geofiltration and hydrodynamic schematization of natural conditions was carried out, and a mathematical model was substantiated that simplifies but reliably reflects natural hydrogeological processes.

The modeling area is the area of the Karakata groundwater deposit, the dimensions of which from the outlets of the productive aquifer are approximately 60 km×60 km.

Geofiltration schematization is reflected in the map of water permeability distribution across the area (Figure 2). It serves as the geofiltration basis of the model and is corrected during the process of solving epignostic problems.The hydrodynamic schematization of the filtration field in the form of pressure distribution within the field area, which serves as the initial basis for comparing natural and model pressures, assessing the adequacy of the model, and calibrating it, is reflected in piezoisogips maps (Fig. 4)

Simulation of the groundwater filtration process on a model requires the specification of external and internal boundary conditions.

The main external boundaries are (Fig. 4):

- filtration feeding of groundwater from the north, northwest;
- filtration feeding of groundwater from the south, southeast.

The outer boundaries of the filtration zone are the areas where productive water-bearing complex deposits emerge to the earth's surface or the boundaries of its contact with Paleozoic formations. In areas where the complex is in contact with the clay deposits of the turon, which is its waterproofing, and where groundwater replenishment is practically absent, the absence of inflow is assumed in the form of setting the boundary condition of type II (GU-II) with the condition Q=0. In areas where groundwater inflow from the Paleozoic fractured zone can be expected, a boundary condition of type II with the condition $Q \neq 0$ is adopted.

Similar boundary conditions are adopted on the contours of the basin's eastern and southeastern boundaries, from where groundwater flows into the basin from the Nuratov and Karatau mountains. Implementation on the groundwater feeding model is carried out by setting boundary condition nets of type I (GU-I) in the form of a constant pressure within a certain time period. The change (decrease) of the head is regulated in the process of solving reverse and predictive problems based on the condition of constant flow from the considered boundary, which should not increase under the influence of operation.

The main internal boundaries are (Fig. 4):

- filtration feeding of groundwater through faults;
- filtration losses from the aquifer through wedging into the upper horizons;
- operational extraction of groundwater.

The inner boundaries of the filtration zone are defined by the zones of water-conducting faults, through which the groundwater of the Paleozoic foundation is discharged into the productive aquifer complex through the weakened zones of its base. The internal boundaries adjacent to the faults must reflect the main feeding of groundwater due to the inflow from them and are given by constant feeding, i. e., II-type GW.

A similar process of upward discharge along these zones is observed in

the roof of the complex, where the groundwater of the complex flows into the above-lying water-bearing complexes, subsequently expending it for the model by assigning III-type boundary conditions (GU-III) that fall within the fault development zones, providing for the dependence of flow rate (Q) on the pressure difference (ΔH) $-\ Q\ =\ f\ (\Delta H)$.

Temporary schematization was determined by the need to solve the epignostic problem against the backdrop of existing water intakes with approved groundwater reserves. When solving inverse problems, the time step is taken from 1 year to 5 years.

3. Result and Discussions

Assessment of model reliability was carried out based on solving inverse stationary and epignostic problems. Their ultimate goal is to calibrate and justify a reliable, adequate natural model that satisfactorily reflects the main elements of the hydrogeological process manifested in the deposit (based on the low informativeness of available data, especially those characterizing the amount of groundwater taken over the last 50-55 years for the basin as a whole).

The criterion for the reliability of the mathematical model is the correspondence of actual and model values of pressures across the entire filtration field under given external and internal boundary conditions, reflecting the real processes of groundwater supply and discharge of the complex.

The most reliable information on the groundwater state of the complex is characterized by 1964, which reflects the position of the piezometric surface of the groundwater, taking into account the existing operation during the period 1957-64, built on more than 40 observation wells. This period was taken as the initial period and reproduced on the model when solving the inverse stationary problem. Based on the comparison of actual and model pressure values, the model was calibrated.

The error of the model head from the actual head was taken as no more than ±5.0m.

Then, the inverse non-stationary problem, consisting of modeling the operation process of the entire Karagatin deposit starting from 1964, was solved. When solving the non-stationary epignostic problem:

- The reliability of the external and internal boundary assignments was assessed, and their adjustments were made; the most labor-intensive was the calibration of the model in the fault zone, through which groundwater discharge is carried out;
- the values of the filtration field's water permeability have been specified, which have changed compared to the water permeability map based on individual sections, typically confined to groundwater discharge zones.

The solution of the stationary problem showed close correspondence between the actual and model values of pressure distribution across the area. For most control wells, the difference in these indicators did not exceed ±5m (Table 4).

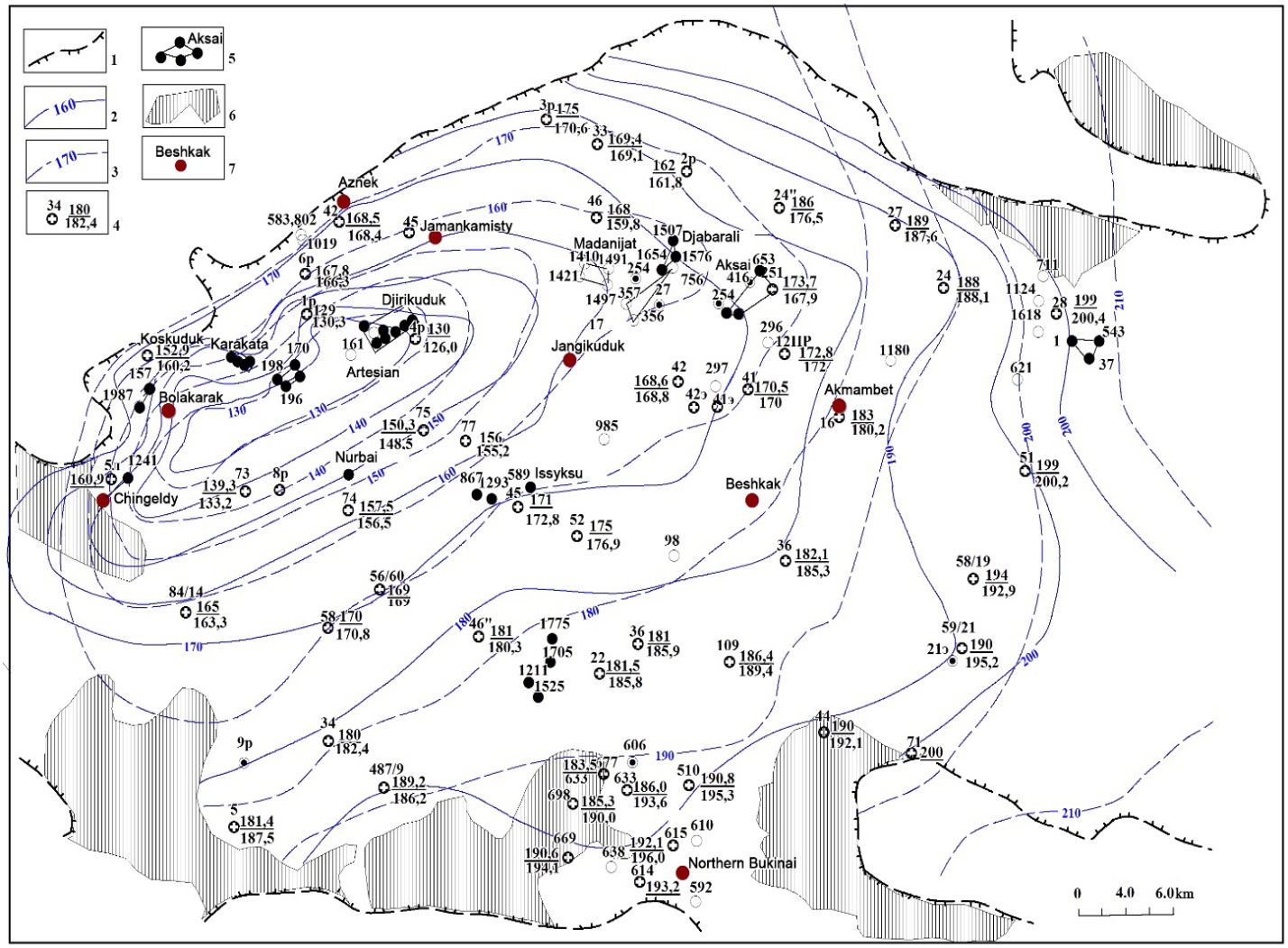

Figure 4: Map of hydroisohypses of the Senon-Lower Oocene complex. 1 - distribution boundary of the Senonian-Lower Eocene aquifer complex; 2 - isolines of the piezoisohypses of the Senon-Lower Oocene complex as of November 1964 (actual), m; 3 - also - according to the modeling data, m; 4 - observation well of the Zarafshan Hydroelectric Power Plant at the top - well number on the right: in the numerator - actual pressure (1964g) in the denominator - pressure according to the modeling data; 5 - water intake; 6 - outcrops of the Senonian-Lower Eocene aquifer complex; 7 – settlement.

Table 4: Actual groundwater levels and their model values according to the data solutions of the inverse problem

No	№ well	H fact.	H model.	ΔH
1964 y				
1	1p	129	138.9	-10.9
2	2p	162	166.2	-4.2
3	3p	169.40	166.20	3.20
4	4p	130	122.8	7.2
5	6p	167.8	166.9	0.9
6	5	181.4	182.8	-1.4
7	12pr	172.8	174.3	-1.5
8	16	183	181.6	1.4
9	22	181.5	179.9	1.6
10	24	188	188.7	-0.7
11	24	186	176.7	9.3
12	27	189	188.1	0.9
13	28	199	200.2	-1.2
14	33(50)	169.4	166	3.4
15	33	171	175	-4
16	34	180	178.8	1.2
17	36	181	180.7	0.3
18	36	182.1	182	0.1
19	41	170.5	174.1	-3.6
20	42	168.6	169	-0.4
21	44	190	188.5	1.5
22	45	184	174.4	9.6
23	46	168	161.8	6.2
24	46	181	176.5	4.5
25	51	199	199.9	-0.9
26	52	175	172.4	2.6
27	58/19	194	191.3	2.7
28	56/60	158	158.9	-0.9
29	58	170	171.3	-1.3
30	59/21	190	192.8	-2.8
31	73	139.3	137.2	2.1
32	74	157.5	156.3	1.2
33	75	150.3	147.4	2.9
34	77	156	154.7	1.3
35	84/14	165	168.5	-3.5
36	109	186.4	184	2.4
37	487/9	189.2	183.5	5.7
38	510	190.8	186.4	4.4

Table 4 (Cont): Actual groundwater levels and their model values according to the data solutions of the inverse problem				
39	633	186	185.1	0.9
40	669	190.6	185.7	4.9
41	698	185.3	183.2	2.1
42	Aksay	173.7	167.9	5.8
43	Akmambet	183	181.6	1.4
44	Koskuduk	162.9	166.3	-3.4
2018 y				
1	3p	140.46	143.1	-2.64
2	4p	124.37	123	1.37
3	6p	146.34	145.9	0.44
4	8p	143.04	139.3	3.74
6	27	135.02	132.1	2.92
7	416	150.24	145.5	4.74
8	638	191.19	184.7	6.49

This convergence of pressures confirms the correct formulation of boundary conditions and filtration field characteristics and the overall reliability of the model. As a result of solving the epignostic problem, the groundwater balance was obtained (Table 5).

Table 5: Balance of underground waters of the Karakata SPV based on the results of solving inverse problems.					
No	**Receipts**	**1964 y.**		**2018 y.**	
		m³/day	**l/s**	**m³/day**	**l/s**
1	Capacitive reserves	0	0	4323	50.03
2	Lateral inflow (s., s-z)	21090	244.10	26610	307.99
3	Lateral tributary (south, south-east)	28739	332.63	35886	415.35
4	Fracture feeding	50058	579.38	50058	579.38
	Total	99887	1156.10	116877	1352.74
	Expenditure items	m³/day		m³/day	
1	Capacitive reserves	0	0	6115	70.78
2	Expl. Selection	49622	574.33	44553	515.66
3	Outflow to the upper mountains.	70057.57	810.85	56294	651.55
Total		119675.86	1385.14	106962	1237.99

The groundwater balance of the complex is generally quite close to the preliminary estimates of dynamic (flow) reserves, which were previously made and estimated at 1.5-1.7 m3/s and obtained from the modeling data of the Karakata deposit during the assessment of the operational reserves of the "Jiri-kuduk" section. According to the modeling data, the flow reserves within the aquifer complex itself are 576.73 l/s, the attracted Paleozoic reserves are 579.38 l/s, or 1156 l/s (1.156 m3/s) for the entire complex under consideration. These figures seem more realistic compared to those previously presented.

However, their reliability, especially the figures of attracted groundwater reserves of the Paleozoic, is not sufficiently high due to the lack of information.

The obtained picture of the hydrogeological process for 1964 was the basis for considering changes in the groundwater state of the complex.

In the process of solving the epignostic problem, the following was considered:

- changes in pressures and balance over several time stages.

The limited number of control wells does not allow for detailed determination of the head position across the entire SPC area. However, the available information set indicates a satisfactory convergence of actual and model pressure values (primarily 1-3m). The graph of the relationship between actual and model pressures at the control points is shown in Figure 5.

The correlation coefficient of dependence of model (Nm) and actual (Nf) pressure values was 0.96 for the stationary problem and 0.95 for the epignostic non-stationary problem. Such a high value of the correlation coefficient confirms the reliability of the obtained mathematical model.

The groundwater balance (Table 5) is characterized by the preservation of feed values (flow reserves) within the previous limits (1.1-1.2 m3/s) with an increase in the depletion of capacitive (elastic) reserves (up to 0.19-0.294 m3/s) when the total value of natural and artificial discharge exceeds. Conversely, exceeding the power supply over the total unloading leads to pressure stabilization and even an increase in individual section

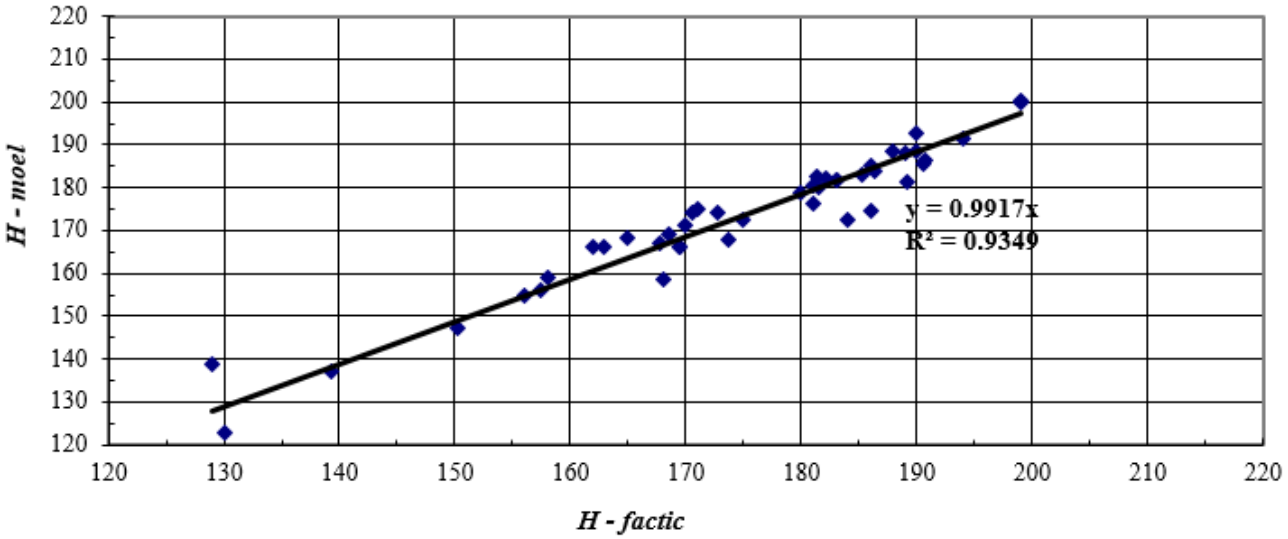

a)

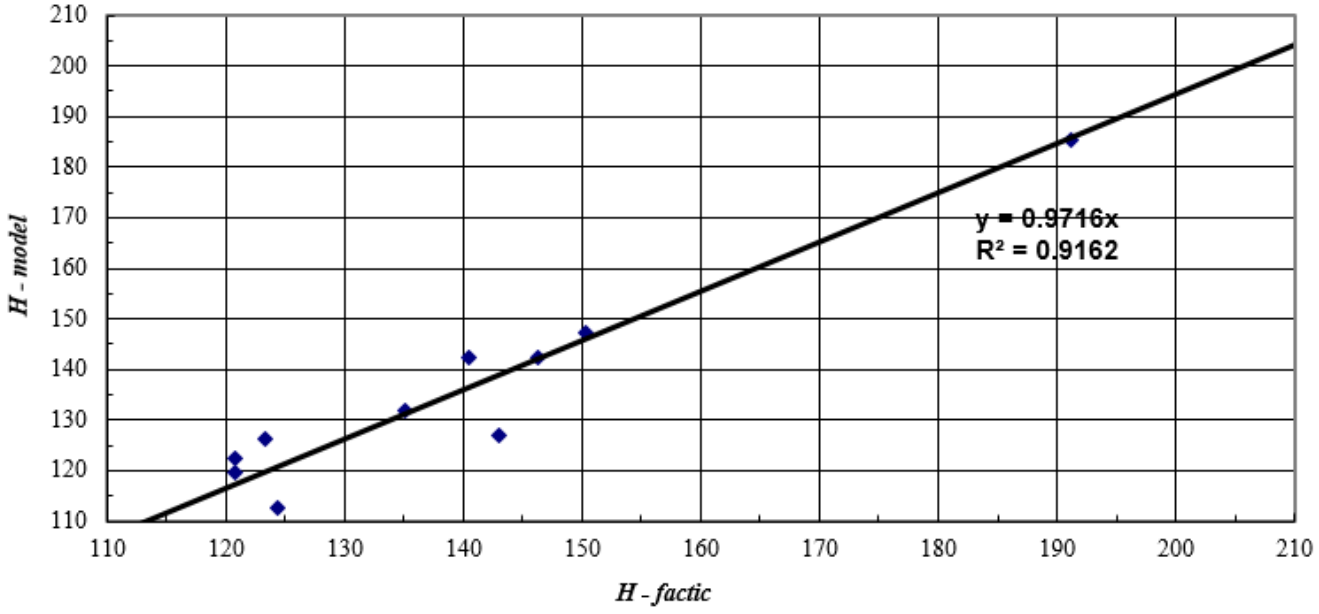

b)

Figure 5: Graph of the relationship between actual and model pressures at control points: a) 1964; b) 2018.

The diagram (Figure 6) reflects changes in the balance structure.

Overall, the completed solutions of the inverse (epignostic) problems sufficiently convincingly demonstrate the adequacy of the numerical model of the natural model.

Thus, the reliability of the presented numerical model of the Karagatin GWD can be considered conditionally proven relative to the adequacy of the natural numerical model.

3. Conclusion

The Senonian-Lower Eocene aquifer complex is developed practically throughout the entire territory of the Karakata Artesian Basin and is exposed on the surface in its mountainside. In the development area, its integrity is disrupted by faults that serve as both suppliers, accumulators, shielders, and drainers of groundwater.

The pressure value above the roof of the aquifer complex varies from 30 to 450 m. The area of self-flowing waters in 1959 was 5200 sq. km (5600 sq. km of the total area).

The formation of natural groundwater reserves of the complex occurs through underground runoff from the surrounding basin of mining structures and underground inflow from the fault zone.

Natural resources in the amount of 138.6 thousand m3/day were calculated in 1969, and in 2004 in the North-Eastern Kyzylkum HGP, they were recalculated using the balance method and estimated at 124.16 thousand m3/day. According to previous studies (Abdullaev et al., 2023)., 471 l/s of dynamic reserves are formed due to the infiltration of atmospheric precipitation into Paleozoic rocks and the complex at its outcrops, which is unlikely and impossible to prove. In addition, they also assessed the additional feeding due to the inflow of groundwater from the Arasai depression in an amount of about 350 l/s and the Tashkurin depression - about 150 l/s, i.

e., the inflow of artesian water balance items was estimated at 971 l/s. The unaccounted feeding of the water-bearing complex, equal to about 700 l/s, was attributed to the fault zone, as evidenced by the high-water temperature in the northern part of the basin. Overall, the dynamic groundwater reserves of the complex are estimated at 1.6-1.7 m3/s.

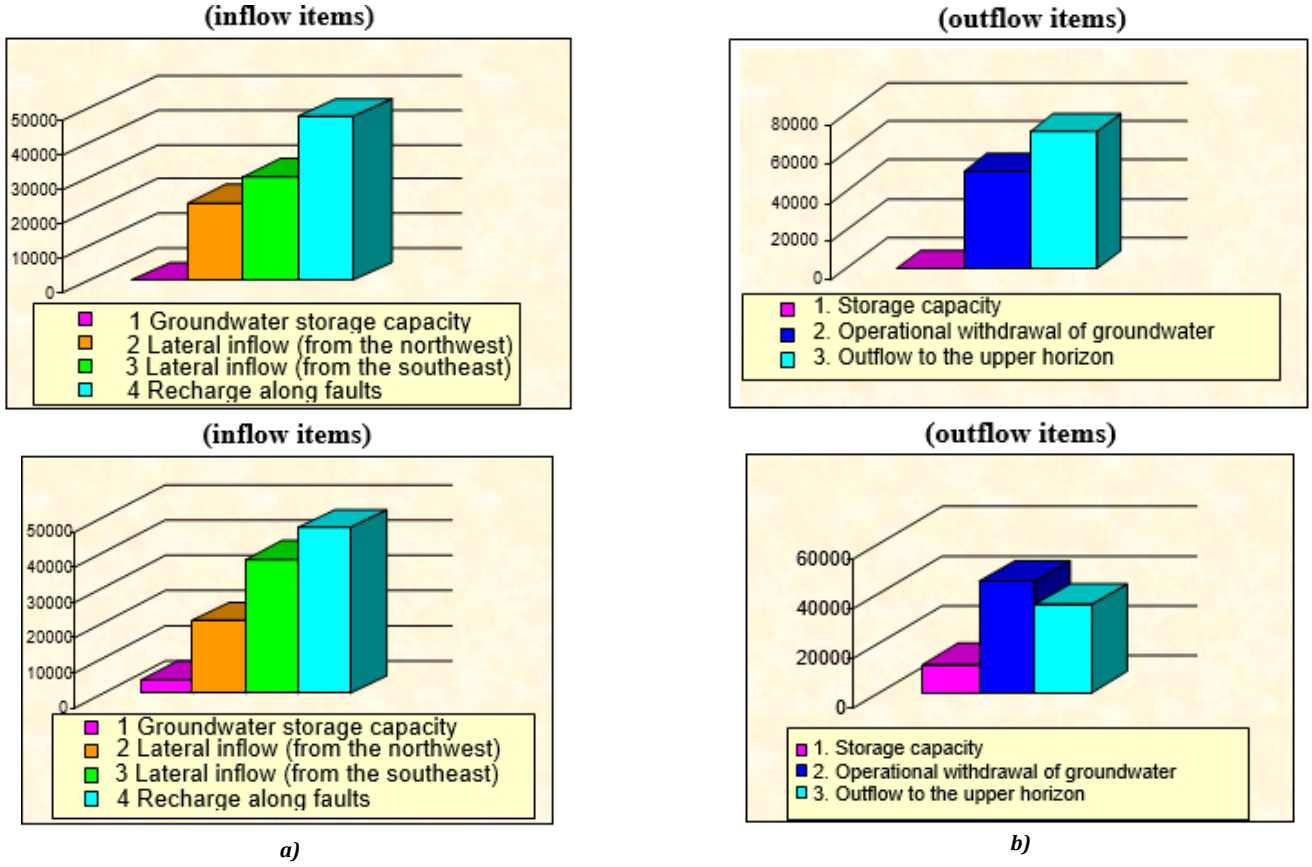

Figure 6: Diagram of the underground water balance components of the Karakata aquifer according to the solution of the inverse problem:

a) 1964 y; b) 2018 y.

According to the modeling data carried out within the framework of these studies, the total dynamic reserves within the MPC do not exceed 1.1–1.2 m^3/s, of which about 0.5 m^3/day falls on the inflow through faults from the Paleozoic. From 1969 to the present, continuous operation of the described water-bearing complex has been carried out, and at the same time, the total average annual selection for the basin changed from 55.73 to 119.0 thousand m^3/day, while in 2004–2018 it decreased to 38.0 thousand m^3/day. During the period of maximum water intake, the area of self-flowing has decreased by no more than 25%, and self-flowing wells are operating at each water intake; if in 1993 out of the total intake (76.52 thousand m^3/day) self-flow was 55.79 thousand m^3/day (73%), then in 2004 out of 47 thousand m^3/day it amounted to 42.6 thousand m^3/day (90%). The well levels did not decrease below ground level and mainly maintained their position from 5 to 30 m above ground level on average, while the processing of piezometric levels in various sections of the basin during the period from 1960 to 2018 was about 10–40 meters. Taking into account that during the sampling, 119 thousand m^3/day (1991y.) and 38.0 thousand m^3/day (2018y.) in the discharge zone, self-flow persisted, it can be asserted that the extraction of groundwater within the Karakata GWD is provided by dynamic and elastic reserves.

REFERENCES

Abdullaev, B. D., Razzakov, R. I., Okhunov, F. A., and Nasibov, B. R., 2023. Modeling of hydrogeological processes in irrigation areas based on modern programs. In E3S Web of Conferences (Vol. 401, p. 02006). EDP Sciences.

Akhtar, N., Syakir, M. I., Anees, M. T., Qadir, A., and Yusuff, M. S., 2020. Characteristics and assessment of groundwater. In Groundwater management and resources. IntechOpen. DOI: 10.5772/intechopen.93800

Brodie, R., Sundaram, B., Tottenham, R., Hostetler, S., and Ransley, T., 2007.

Engineering Geological, and Hydrogeological Aspects. Water Resources, 49 (Suppl 2), S59-S68.

Hafezifar, E., Shourian, M., 2025. Groundwater level prediction using deep learning-based recurrent neural network and numerical modeling: a comparative study. Earth Science Informatics, 18(2), Pp. 1-18.

An overview of tools for assessing groundwater-surface water connectivity. Bureau of Rural Sciences, Canberra, Australia, 131.

Carrera, J., Alcolea, A., Medina, A., Hidalgo, J., Slooten, L. J., 2005. Inverse problem in hydrogeology. Hydrogeology journal, 13(1), 206-222. DOI 10.1007/s10040-004-0404-7

Chen, Y., Zhang, Y., Xia, F., Xing, Z., and Wang, L., 2022. Impacts of underground reservoir site selection and water storage on the groundwater flow system in a mining Area - A case study of daliuta mine. Water, 14(20), 3282. https://doi.org/10.3390/w14203282

Chesnaux, R., Lambert, M., Walter, J., Fillastre, U., Hay, M., Rouleau, A., and Germaneau, D., 2011. Building a geodatabase for mapping hydrogeological features and 3D modeling of groundwater systems: application to the Saguenay–Lac-St.-Jean region, Canada. Computers and Geosciences, 37(11), Pp. 1870-1882. https://doi.org/10.1016/j.cageo.2011.04.013

Choi, C. C., and Mantilla, R., 2015. Development and analysis of GIS tools for the automatic implementation of 1D hydraulic models coupled with distributed hydrological models. Journal of Hydrologic Engineering, 20(12), 06015005. https://doi.org/10.1061/(ASCE)HE.1943-5584.0001202

Djumanov J.Kh., Hushvaktov S.H., Anorboyev E.A., Ma'mirov F.A., 2021. Application geoinformational technologies in hydrogeological research. Intyernational confyerence.. ICISCT 2021, Tashkent. https://ieeexplore.ieee.org/document/9670406

Djumanov J.Kh., Hushvaktov S.H., Yakhshibaev R., Sayfullaeva N., 2021. Mathematical model and software package for calculating the balance of information flow. ICISCT 2021. https://ieeexplore.ieee.org/author/37089246048

Funikova, V. V., Dudler, I. V., and Butaev, R. T., 2022. Anthropogenic Changes in the Groundwater Regime of Built-Up Areas: Geoecological,

Harne, S., Chaube, U. C., Sharma, S., Sharma, P., and Parkhya, S. 2006. Mathematical modelling of salt water transport and its control in groundwater. Nature and Science, 4(4), Pp. 32-39.

Henshaw, P. C., Charlson, R. J., and Burges, S. J., 2000. Water and the hydrosphere. In International geophysics Vol. 72, Pp. 109-131. Academic Press. https://doi.org/10.1016/ S0074-6142(00)80112-6

Jamali, S., Punthakey, J. F., Ahmed, W., Qureshi, A. L., Raheem, A., Mitchell, M., and Ahmed, M., 2025. Groundwater Modelling Assessment of a Coastal Agriculture Climate Change Adaptation Strategy Incorporating Green Infrastructure: An Indus Delta Case Study. Groundwater for Sustainable Development, 101484.

Kashavarov, A.A., 1998. Mathematical modeling of salt transport processes by interconnected underground and surface water flows. Moscow, 39(4). Pp. 118-126.

Long, D., Yang, W., Scanlon, B. R., Zhao, J., Liu, D., Burek, P., and Wada, Y., 2020. South-to-North Water Diversion stabilizing Beijing's groundwater levels. Nature communications, 11(1), Pp. 3665.

Polshkova, I. 2023. Study of groundwater using hydrodynamic models. In Human-Assisted Intelligent Computing: Modeling, simulations and applications. Pp. 25-1. Bristol, UK: IOP Publishing.

Rasouli, M. M., Ketabchi, H., Mahmoodzadeh, D., 2025. Groundwater-surface water interaction in a river-wetland-aquifer regional system using a coupled simulation-based approach. Journal of Hydrology, 656, 133006.

Shestakov, V., and Nevecherya, I., 2009. Filtration calculations for an imperfect well in a pressureless flow. Bulletin of Moscow University. Geology, 4(6), Pp. 55-59.

Telyma, S., Voloshkina, O., Kovalova, A., and Bereznytska, Y., 2023. Optimization of the building process of ground water intakes under the conditions of natural water resources deficits. Construction with Optimized Energy Potential, 12.

Zaborova, D. D., Kozinec, G. L., Musorina, T. A., and Petrichenko, M. R., 2020. Mathematical model for unsteady flow filtration in homogeneous closing dikes. Power technology and engineering, 54(3), Pp. 358-364. DOI 10.1007/s10749-020-01216-9

Zakir-Hassan, G., Punthakey, J. F., Allan, C., and Baumgartner, L., 2025. Integrating Groundwater Modelling for Optimized Managed Aquifer Recharge Strategies. Water, 17(14), Pp. 2159.